I&EC research
Industrial & Engineering Chemistry Research

Article

pubs.acs.org/IECR

Using Membrane Reactive Absorption Modeling to Predict Optimum Process Conditions in the Separation of Propane−Propylene Mixtures

Marcos Fallanza, Alfredo Ortiz, Daniel Gorri, and Inmaculada Ortiz*

Departamento de Ingeniería Química y Química Inorgánica, Universidad de Cantabria, Avenida de los Castros s/n 39005 Santander, Spain

ABSTRACT: In membrane reactive absorption, a gas mixture is contacted with a liquid absorbent in a membrane module to selectively dissolve one or more components from the gas in the liquid, accompanied by a chemical reaction in the liquid phase. The complexity of modeling multiphase systems increases when mass transfer phenomena take place together with chemical reactions. Therefore, it is very important to have reliable mathematical models for process design and scale up, that describe the phenomena involved in the easiest way possible. We propose the separation of propylene−propane gas mixtures in a hollow fiber contactor as a case study. A thorough mathematical model that accounts for the factors influencing the flux through the membrane: (1) gas flux through the membrane pores, (2) kinetic resistances to mass transfer in both fluid phases, and (3) influence of the chemical reaction on the overall kinetics, is reported. First, the model has been validated through the comparison of simulated results with previously reported experimental data. Second, the effect of the module configuration, parallel flow, and cross-flow as well as flow patterns, cocurrent flow, and countercurrent flow on the performance of the separation process is analyzed. Process simulation showed that significant improvement of the fluid-dynamics can be reached by using a cross-flow membrane contactor and the process performance benefits from a countercurrent operating mode.

1. INTRODUCTION

Most of the reactive absorption processes are carried out using conventional industrial gas−liquid contactors (packed columns, disc contactors, plate column, bubble column, mechanically agitated contactors, spray column, venturi scrubbers, etc.) which achieve mass transfer by direct contact and dispersion of one phase within the other. In most of the dispersive type contactors, mass transfer and interfacial area depend on the process/operation conditions which are the key drivers of the absorption rate of the gaseous components onto the liquid phases. Moreover, conventional gas−liquid contactors can suffer from flooding, weeping, foaming, entrainment, or channeling effects, and they require further separation steps after the main absorption process is finalized.[1,2] Recently, a number of researchers have paid attention to the use of gas−liquid membrane contacting processes (nondispersive contactors) in their application to gas separation. Microporous membrane contactors are systems employed to keep in contact two phases. They do not offer any selectivity for a particular species with respect to another, they simply act as a barrier between the phases involved. These membrane contactors offer numerous advantages over the conventional gas−liquid contactors providing up to 2 orders of magnitude more surface area per volume than conventional contactors.

Some of the main advantages include the following:[2−6]

- The high specific gas−liquid interfacial area for mass transfer remains undisturbed because the two flows are independent, and it is equal to the geometrical membrane surface area.
- In these contactors, the mass transfer coefficients and specific area can be varied independently. Emulsion formation does not occur, again because there is no fluid/fluid dispersion.
- Contamination due to mixing of the phases is avoided.
- Compactness and low weight of structures are achieved. Equipment volume reductions of up to 20% for gas absorption have been reported.[7]
- The scale-up of the membrane contactor is straightforward and simple due to the modular nature of the contactor.
- It is less energy intensive than conventional processes.

However membrane contactors still exhibit some limitations which should be avoided such as (i) appearance of an additional (membrane) mass transfer resistance to the overall mass transfer process, (ii) accurate control of transmembrane pressure, (iii) membrane life, (iv) material compatibility with certain solvents, (v) loss in efficiency due to bypassing and dead zone on the shell side,[2,4] (vi) scarce availability of suitable mathematical models that describe mass transfer phenomena in membrane contactors with specific geometries. Nevertheless, these disadvantages are not always important, and selecting the suitable device geometry and operational conditions can be minimized.

Principally two different types of membranes such as symmetric hydrophobic porous membranes or asymmetric membranes with an ultrathin layer can be used in gas−liquid membrane contactors. In both cases, the membrane must be able to separate the contacting fluids.[7,8] Typical membranes are prepared from hydrophobic polymer materials possessing a high porosity, a membrane thickness of 10−300 μm, and providing microfiltration properties with pore size of 0.1−1 μm.[5] The choice of the membrane material affects phenomena such as sorption and chemical stability under conditions of actual application.

Special Issue: Giulio Sarti Festschrift

Received: September 25, 2012
Revised: January 9, 2013
Accepted: January 11, 2013
Published: January 11, 2013

dx.doi.org/10.1021/ie302614r | *Ind. Eng. Chem. Res.* 2013, 52, 8843−8855

Hydrophobic polymers, polypropylene (PP), polyethylene (PE), polytetrafluoroethylene (PTFE), and polyvinylidene fluoride (PVDF) are the most popular membrane materials because they have excellent chemical and thermal resistances.[5,9] Alternatively, inorganic membranes can be also used providing, in some cases, better chemical and thermal stability as well as high mechanical strength. However, most ceramic materials are hydrophilic in nature, and surface modification is required to improve their hydrophobicity;[5] in addition, inorganic membranes are more expensive than polymeric membranes. Critical issues to consider in the design of membrane contactor processes are the geometry of the membrane contactor and the mode of operation. Accordingly, these devices can be broadly classified into (i) flat sheet membranes (plate and frame or spiral wound membrane contactors) and (ii) hollow fiber membrane contactors which can be used in parallel flow mode (cocurrent or countercurrent) or cross-flow mode in order to improve the shell side mass transfer coefficients.[2,10]

Many works in the literature have focused on gas/liquid mass transfer occurring within hollow fiber membrane contactors, especially for CO_2 capture,[6,11−16] hydrogen sulfide odor control,[17] removal of acid gases,[18,19] high pressure gas treating processes such as natural gas or ammonia recovery from off gas streams.[20]

Process simulation can lead to better insight in process understanding. The mathematical modeling of the physical absorption taking place in a membrane contactor has been addressed in many research works. Interesting works have also analyzed the effect of membrane partial wetting; however, the mathematical description of chemical absorption in gas−liquid membrane contacting processes and their experimental validation in the open literature is very limited.[6,10,15,21−24] The modeling of this complex operation requires an adequate modeling framework. In chemical absorption processes, the transfer of the reactive compound from the gas phase into the liquid phase during absorption is governed by two limiting factors: (1) mass transfer limitations and (2) reaction kinetic limitations. The former is dependent on the solution containing the dissolved reactive absorbent and the process equipment used, while the latter is dependent only on the solution containing the dissolved reactive absorbent. For a better performance, both factors have to be taken into account, i.e. fast mass transfer and fast kinetics. The mass transfer characteristics are usually dependent on the diffusivities and fluid mixing, geometries, etc., of the equipment used. The kinetic characteristics are dependent on the type(s) of reactive chemical(s) being used and the solvent in which they are dissolved. The absorption performance of an absorbent can be expressed in terms of an enhancement factor.[1] The enhancement factor concept is introduced to describe the influence of a reaction on the total mass transfer rate and is defined as the ratio of the rate of absorption of a gas into a reactive absorbent to the rate of the physical process at identical process conditions.[25]

The purpose of the current work is to provide a simple mathematical model able to describe the total mass transfer rate of a reactive absorption process carried out in a gas−liquid membrane contactor device. Mass balances to the fluid phases together with the resistances in series approach and including a reaction enhancement factor constitute the essential elements of the model. In addition, the model has been applied and validated to the separation of propane−propylene gas mixtures as a case of study, showing the performance of different module configuration geometries and modes of operation.

2. MODEL DEVELOPMENT

The design of multiphase equipment such as membrane contactors for gas−liquid absorption is a difficult task due to its highly complex nature.[26] Moreover, among the many different types of multiphase chemical processes, reactive absorption is regarded as one of the most complex systems due to interactions between chemical reaction and mass transfer taking place between the gas and liquid phases. Although many researchers have paid attention to model and optimize reactive absorption equipments, the modeling of these systems is still very challenging due to the high complexity of these systems. Figure 1 shows a schematic diagram of the reactive absorption process of gas A into a liquid using a membrane contactor with gas and liquid phases flowing in countercurrent flow.

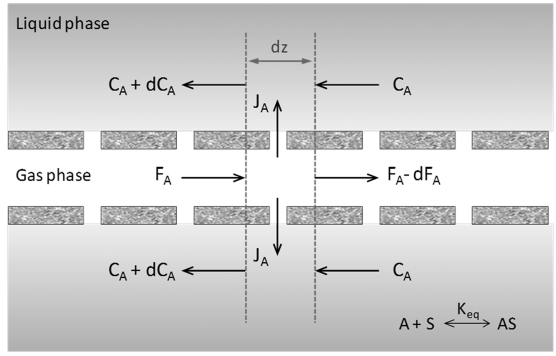

Figure 1. Schematic diagram of the reactive absorption process of gas A into a liquid phase implemented in a membrane contactor with gas and liquid phases in countercurrent flow.

2.1. Mass Balances. In order to develop the mass balances for all the species involved in the gas−liquid absorption process using membrane contactors, these main assumptions were undertaken:

(i) Plug flow and negligible axial diffusion in both phases.
(ii) Each fiber has identical specifications.
(iii) Hollow fibers are hydrophobic, so the pores are completely filled by the gas phase.
(iv) Ideal gas behavior is imposed.
(v) The system is under isothermal operation.

The mass balance for the gas A in the gas phase is given by eq 1:

$$\frac{dF_A}{dz} = -\frac{A}{L}J_A \tag{1}$$

with boundary condition

$$z = 0 \Rightarrow F_A = F_{A,IN}$$

where F_A is the molar flow rate of the gas A in the gas phase, z is the axial position in the module, A is the membrane total area, and L is the effective fiber length.

The mass balance for the gas A in the liquid phase can be expressed as

$$\frac{V}{Q_L L}\frac{\partial C_A}{\partial t} + \frac{\partial C_A}{\partial z} = \frac{A}{Q_L L}J_A \tag{2}$$

with initial and boundary conditions

$$t = 0 \Rightarrow C_A = 0$$

$$z = 0 \Rightarrow C_A = 0 \quad \text{for gas and liquid flowing in cocurrent flow}$$

$$z = L \Rightarrow C_A = 0 \quad \text{for gas and liquid flowing countercurrently}$$

dx.doi.org/10.1021/ie302614r | Ind. Eng. Chem. Res. 2013, 52, 8843−8855

Table 1. Summary of Correlations to Calculate the Mass Transfer Coefficient in the Shell Side for Parallel Flow and Transverse Flow Membrane Contactors

reference	correlations for parallel flow membrane contactors	conditions
Yang and Cussler[31]	$Sh = 1.25\left(\frac{d_h^2 u}{L\nu}\right)^{0.93}\left(\frac{\nu}{D_{C3H6,l}}\right)^{1/3}$ (11)	$0.5 < Re < 500$ $0.03 < \phi_F < 0.26$
Prasad and Sirkar[32]	$Sh = 5.8\left[(1-\phi_F)\frac{d_h}{L}\right]\left(\frac{d_h u}{\nu}\right)^{0.6}\left(\frac{\nu}{D_{C3H6,l}}\right)^{1/3}$ (12)	$0 < Re < 500$ $0.04 < \phi_F < 0.4$
Wu and Chen[33]	$Sh = (0.3045\phi_F^2 - 0.3421\phi_F + 0.15)\left(\frac{d_h u}{\nu}\right)^{0.9}\left(\frac{\nu}{D_{C3H6,l}}\right)^{1/3}$ (13)	$32 < Re < 1290$ $0.08 < \phi_F < 0.70$
Costello et al.[34]	$Sh = (0.53 - 0.58\phi_F)\left(\frac{d_h u}{\nu}\right)^{0.53}\left(\frac{\nu}{D_{C3H6,l}}\right)^{1/3}$ (14)	$21 < Re < 324$ $0.32 < \phi_F < 0.76$
Li et al.[35]	$Sh = 1.164\left(\frac{d_h^2 u}{L\nu}\right)^{0.967}\left(\frac{\nu}{D_{C3H6,l}}\right)^{1/3}$ (15)	$20 < Re < 500$ $0.04 < \phi_F < 0.20$
reference	correlations for transverse flow membrane contactors	conditions
Zheng et al.[36]	$Sh = 2.15\left(\frac{d_h u}{\nu}\right)^{0.42}\left(\frac{\nu}{D_{A,l}}\right)^{1/3}$ (16)	$0.8 < Re < 20$ $0.40 < \phi_F < 0.46$
Fouad et al. (Modif)[37]	$Sh = 0.41\left(\frac{d_h u}{\nu}\right)^{0.36}\left(\frac{\nu}{D_{A,l}}\right)^{1/3}$ (17)	$0.1 < Re < 0.4$
Schöner et al.[38]	$Sh = 1.76\left(\frac{d_h u}{\nu}\right)^{0.82}\left(\frac{\nu}{D_{A,l}}\right)^{1/3}$ (18)	$0.02 < Re < 5$ $0.49 < \phi_F < 0.53$
Baudot et al.[39]	$Sh = 0.56\left(\frac{d_h u}{\nu}\right)^{0.62}\left(\frac{\nu}{D_{A,l}}\right)^{1/3}$ (19)	$0.02 < Re < 30$ $0.49 < \phi_F < 0.53$
Shen et al.[40]	$Sh = 0.055\left(\frac{d_h u}{\nu}\right)^{0.72}\left(\frac{\nu}{D_{A,l}}\right)^{1/3}$ (20)	$0.1 < Re < 250$ $0.32 < \phi_F < 0.45$
Fallanza et al.[41]	$Sh = 1.1\left(\frac{d_h u}{\nu}\right)^{0.32}\left(\frac{\nu}{D_{A,l}}\right)^{1/3}$ (21)	$0.003 < Re < 0.006$ $\phi_F = 0.45$

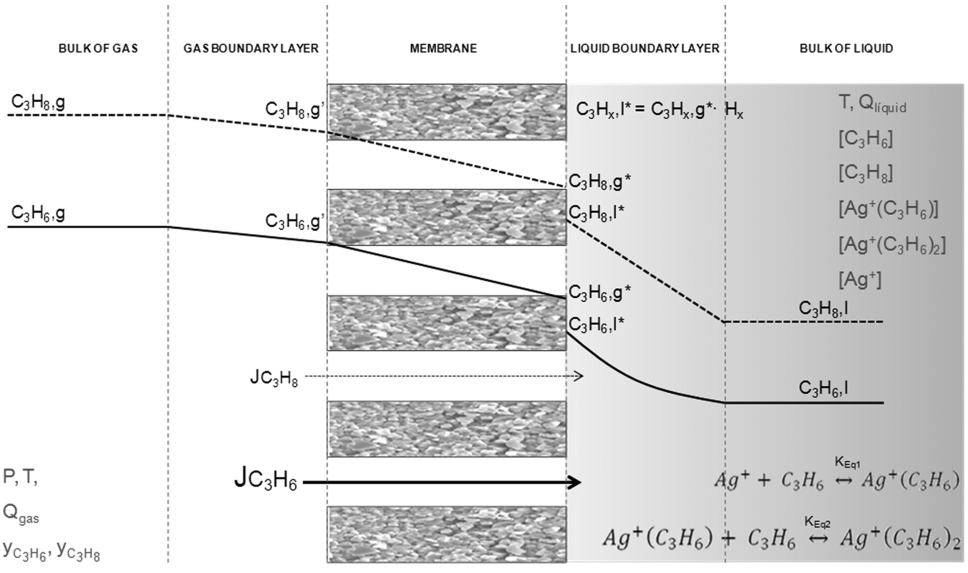

Figure 2. Absorption mechanism of propane and propylene with the resistances in series approach in a nonwetted membrane contactor.

where V is the volume of the liquid side of the membrane contactor, Q_L is the liquid flow rate, and C_A is the concentration of gas dissolved in the liquid flowing through the module. These material balances are coupled by the flux of gas through the membrane, which can be expressed as a function of the driving force (difference in propylene concentrations between

dx.doi.org/10.1021/ie302614r | Ind. Eng. Chem. Res. 2013, 52, 8843−8855

Table 2. Values of the Model Parameters and Constants

parameter	value
$H_{298K,C3H6}$ (mol L^{-1} bar^{-1})	0.069
$H_{0,C3H6} \times 10^6$ (mol L^{-1} bar)	4.61
$\Delta H_{sol,C3H6}$ (kJ mol^{-1})	−23.9
$H_{298K,C3H8}$ (mol L^{-1} bar^{-1})	0.028
$H_{0,C3H8}$ (mol L^{-1} bar)	0.166
$\Delta H_{sol,C3H8} \times 10^6$ (kJ mol^{-1})	−29.8
$D_{Kn,C3H6} \times 10^5$ (m^2 s^{-1})	2.58
$D_{b,C3H6} \times 10^6$ (m^2 s^{-1})	7.52
$D_{g,C3H6} \times 10^6$ (m^2 s^{-1})	5.83
$D_{Kn,C3H8} \times 10^5$ (m^2 s^{-1})	2.52
$D_{b,C3H8} \times 10^6$ (m^2 s^{-1})	7.52
$D_{g,C3H8} \times 10^6$ (m^2 s^{-1})	5.8
$D_{l,C3H6}^{BMImBF4\_0M} \times 10^{10}$ (m^2 s^{-1})	1.88
$D_{l,C3H6}^{BMImBF4\_0.1M} \times 10^{10}$ (m^2 s^{-1})	1.82
$D_{l,C3H6}^{BMImBF4\_0.25M} \times 10^{10}$ (m^2 s^{-1})	1.46
$D_{l,C3H8}^{BMImBF4\_0M} \times 10^{10}$ (m^2 s^{-1})	1.73
$D_{l,C3H8}^{BMImBF4\_0.1M} \times 10^{10}$ (m^2 s^{-1})	1.68
$D_{l,C3H8}^{BMImBF4\_0.25M} \times 10^{10}$ (m^2 s^{-1})	1.35
$D_{Ag^+-BMImBF4} \times 10^{10}$ (m^2 s^{-1})	1.68
$D_{Ag^+-BMImBF4\_0.1M} \times 10^{10}$ (m^2 s^{-1})	1.79
$D_{Ag^+-BMImBF4\_0.25M} \times 10^{10}$ (m^2 s^{-1})	1.99
K_{eq1}(298 K) (L mol^{-1})	245.1
ΔH_{r1} (kJ mol^{-1})	−11.0
K_{eq2}(298 K) (L mol^{-1})	5.9
ΔH_{r2} (kJ mol^{-1})	−38.7
$k_{C3H6-Ag+}$ (L mol min^{-1})	35000

Table 3. Characteristics of the Tubular Membrane Module MD020 TP 2N as Supplied by Enka-Microdyn

MICRODYN MD020 TP 2N	
membrane material	polypropylene
housing material polypropylene	polypropylene
inner diameter of the shell (m)	0.02
inner diameter of the fibers (m)	5.5×10^{-3}
outer diameter of the fibers (m)	8.6×10^{-3}
wall thickness (m)	1.55×10^{-3}
nominal pore diameter (m)	0.2×10^{-6}
porosity (%)	75
number of fibers	3
module length (m)	0.75
effective membrane area (m^2)	0.036
mass of polypropylene membrane (kg)	0.016
packing factor	0.55
tortuosity	1.4

the gas phase and the liquid bulk) and the overall mass transfer coefficient (eq 3):

$$J_A = K_{overall}\left(\frac{P_T y_A}{RT} - \frac{C_A}{HRT}\right) \quad (3)$$

where J_A is the flux of the gas A across the membrane (mol m^2 s^{-1}), $K_{overall}$ is the overall mass transfer coefficient (m s^{-1}), P_T is the total pressure of the gas phase (bar), y_A is the molar fraction of the gas A in the gas phase, R is the constant of ideal gases (bar m^3 mol^{-1} K^{-1}), T is the temperature of the system (K), H is the Henry's constant (mol L^{-1} bar^{-1}), and C_A is the concentration of the gas A in the liquid phase (mol L^{-1}).

2.2. Mass Transfer. In membrane gas−liquid contacting processes, the gas solute has to diffuse from the bulk of the gas phase across the membrane to the bulk of the liquid phase. So that there are three main resistances to mass transfer located in the gas phase, membrane, and liquid phase boundary layers that must be considered.[3,27,28] In this case, the resistances-in-series approach can be used to describe the mass transfer phenomena. Taking into account that the mass transfer between gas and liquid takes place in the gas−liquid interface, and considering hydrophobic membranes, the resistances-in-series can be written for (a) the liquid flowing through the shell side and (b) liquid flowing through the lumen of the fibers, as eqs 4 and 5, respectively:

$$\frac{1}{K_{overall}} = \frac{d_{out}}{k_g d_{in}} + \frac{d_{out}}{k_{mg} d_{lm}} + \frac{1}{k_l H_{di} E_A} \quad (4)$$

Table 4. Operating Conditions Used to Validate the Mathematical Model

ionic liquid	$BMImBF_4$
gas flow rate (mL min^{-1})	16.66
gas pressure (bar)	1
inlet gas composition (%v/v C_3H_6/C_3H_8)	0−100/100−0
liquid flow rate (mL min^{-1})	300−900
liquid pressure (bar)	1.2
[Ag^+] (mol L^{-1})	0−0.25
temperature (K)	298

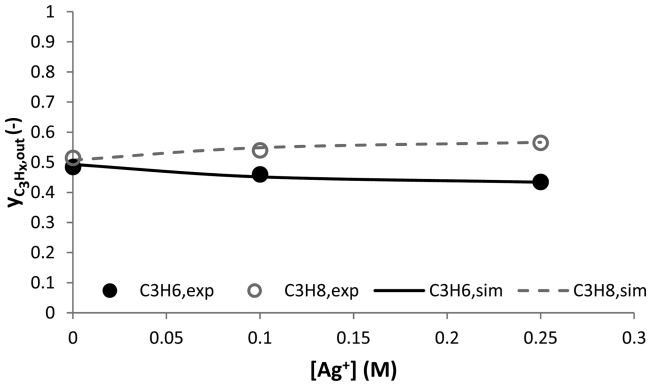

Figure 3. Comparison between experimental and simulated results at different silver concentrations (0−0.25 M) at a liquid flow rate of 300 mL/min, gas flow rate of 16.66 mL/min, and a feed gas composition of 50% C_3H_6/50% C_3H_8 at 1.2 bar.

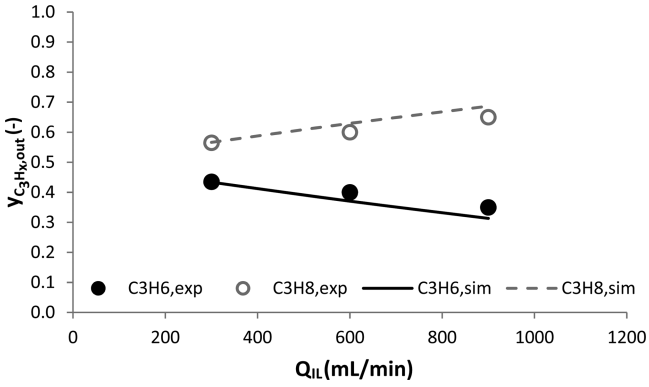

Figure 4. Comparison between experimental and simulated results at liquid flow rates (300−900 mL/min) at a silver concentration of 0.25 M, gas flow rate of 16.66 mL/min, and a feed gas composition of 50% C_3H_6/50% C_3H_8 at 1.2 bar.

dx.doi.org/10.1021/ie302614r | Ind. Eng. Chem. Res. 2013, 52, 8843−8855

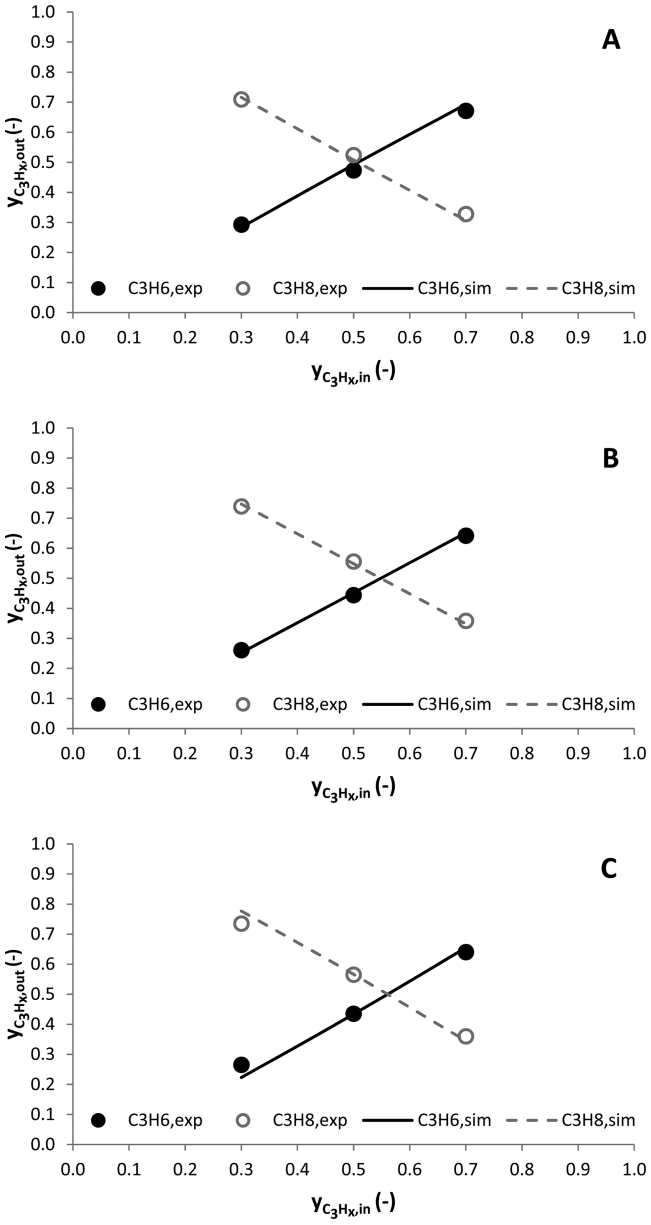

Figure 5. Comparison between experimental and simulated results at feed gas compositions (30−70% C_3H_6), with a liquid flow rate of 300 mL/min, a gas flow rate of 16.66 mL/min at 1.2 bar at silver salt concentrations of (A) 0, (B) 0.1, and (C) 0.25 M.

$$\frac{1}{K_{overall}} = \frac{1}{k_g} + \frac{d_{in}}{k_{mg} d_{lm}} + \frac{d_{in}}{k_l d_{out} H_{di} E_A} \tag{5}$$

where $K_{overall}$ is the overall mass transfer coefficient and k_g, k_{mg}, and k_l are the individual mass transfer coefficients of the gas phase, the membrane (when the pores are filled with gas), and the liquid phase, respectively. H_{di} represents the dimensionless Henry's constant while d_{out}, d_{in}, and d_{lm} are the outer, inner, and logarithmic mean diameters of the fibers, and E_A is the enhancement factor which takes into account the improvement in the overall mass transfer rate due to the chemical reaction.

2.2.1. Mass Transfer Coefficient in the Lumen Side. The local mass transfer coefficient in the lumen side can be calculated using different correlations reported in the literature. The expression developed by Lévêque in the restricted range of laminar flow inside the fibers has been widely used (eq 6).[29]

$$Sh = 1.62 + Gz^{0.33} \tag{6}$$

However, the mass transfer rate can be underestimated for low Graetz numbers. Another correlation proposed by Hausen for laminar flow and low Gz number can be used (eq 7):[29,30]

$$Sh = 3.66 + \frac{0.0668Gz}{1 + 0.04Gz^{2/3}} \tag{7}$$

2.2.2. Mass Transfer Coefficient in the Membrane. The mass transfer coefficient in the hydrophobic microporous membrane depends on the diffusion coefficient of the gas in the gas phase inside the pores and on the characteristics of the membrane (eq 8):[4]

$$k_{mg} = \frac{D_{A,g}\varepsilon}{\tau\delta} \tag{8}$$

where ε, τ, and δ are the porosity, tortuosity, and thickness of the membrane, respectively. $D_{A,g}$ is the diffusion of species A in the gas phase inside the pores of the membrane.

2.2.3. Mass Transfer Coefficient in the Shell Side. For membrane contactors with parallel or transverse flow, the mass transfer coefficient in the shell side can be estimated using several correlations available in the literature (Table 1), being d_h the hydraulic diameter defined in eqs 9 and 10 for parallel flow membrane contactors and for transverse flow membrane contactors respectively; $D_{A,l}$ is the diffusion coefficient of species A in the liquid, L is the fiber length, ν is the kinematic viscosity of the liquid, u is the liquid linear velocity, and $\varnothing_F$ is the membrane packing factor.

$$d_h = \frac{d_{cin}^2 - N d_{out}^2}{N d_{out}} \tag{9}$$

$$d_h = \frac{d_{cin}^2 - d_{co}^2 - N d_{out}^2}{N d_{out}} \tag{10}$$

2.3. Physical Properties. The estimation of the physical properties involved in the absorption process such as solubility and diffusivity is one of the most important factors for the mathematical modeling of the absorption process with chemical reaction.

2.3.1. Physical Solubility. When a gas is in contact with a liquid, it is dissolved until gas−liquid equilibrium is established. The concentration at equilibrium of the gas into a liquid is related to its partial pressure by the Henry's constant:

$$H = \frac{C}{P} \tag{22}$$

Henry's constant has an important dependence with temperature which can be described using a van't Hoff-type equation:[42]

$$H = H_0 e^{(-\Delta H_{sol}/RT)} \tag{23}$$

where the parameters H_0 and $-\Delta H_{sol}$ depend on the gas to be absorbed and the liquid solvent.

2.3.2. Diffusivities. The molecular diffusion coefficient of a gas into another ($D_{A,g}$) can be calculated by Fuller's equation (eq 24):[43]

$$D_{A,b} = \frac{0.01013 T^{1.75} \left(\frac{1}{M_A} + \frac{1}{M_B}\right)^{0.5}}{P_T[(\sum \vartheta_A)^{1/3} + (\sum \vartheta_B)^{1/3}]^2} \tag{24}$$

dx.doi.org/10.1021/ie302614r | Ind. Eng. Chem. Res. 2013, 52, 8843−8855

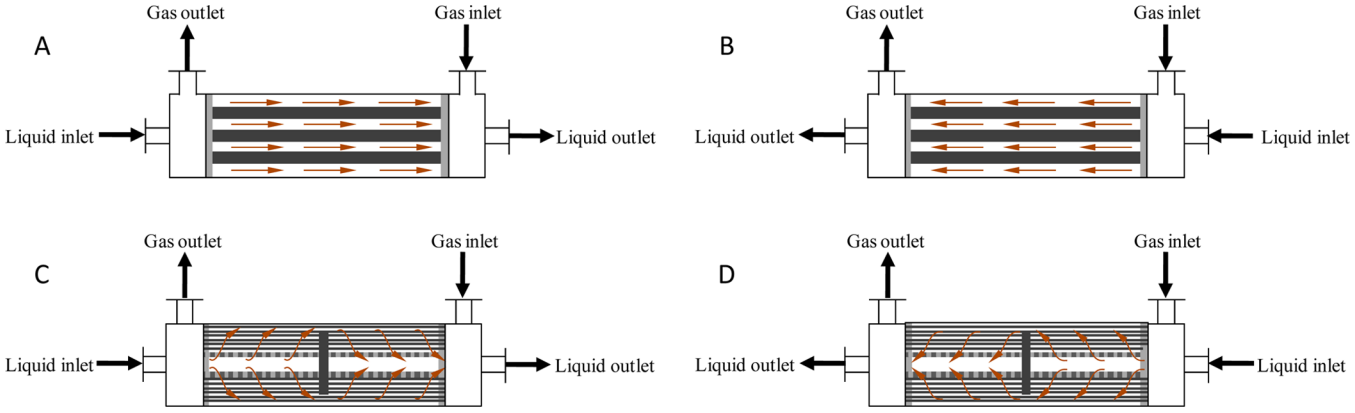

Figure 6. Schematic diagram of the parallel flow membrane contactor with tubular configuration with gas and liquid flowing in parallel (A) and in countercurrent mode (B) and a transversal flow membrane contactor with gas and liquid flowing in parallel (C) and in countercurrent mode (D).

Table 5. Parameters of the Membrane Contactors Used to Make the Performance Comparison between the Tubular Membrane Contactor and the Transverse Flow Membrane Contactor

	tubular parallel flow	hollow fiber transverse flow
inner diameter of the shell (m)	0.02	0.05
inner diameter of the fibers (m)	5.5×10^{-3}	220×10^{-6}
outer diameter of the fibers (m)	8.6×10^{-3}	300×10^{-6}
wall thickness (m)	1.55×10^{-3}	40×10^{-6}
nominal pore diameter (m)	0.2×10^{-6}	0.04×10^{-6}
porosity (%)	75	40
number of hollow fibers	3	10200
module length (m)	28.56	0.16
effective membrane area (m^2)	1.4	1.4
packing density	0.55	0.45
tortuosity	1.4	1.4

Units of T and P are kelvin and pascal, respectively, with the resulting diffusivity in squared meters per second. M_A and M_B are the molecular weights in grams per mole. $\sum\vartheta_A$ and $\sum\vartheta_B$ are the summation of atomic diffusion volumes for gases A and B.

However, the diffusion coefficient of the gas A into the gas B inside the pores of the membrane depends not only on the molecular diffusion, but also on the Knudsen diffusion, which takes into account the fact that the gas molecules frequently collide with the pore wall. Thus, the diffusivity of a gas inside the membrane pores filled by gas is a combination between molecular diffusion and Knudsen diffusion that can be calculated as follows:[44]

$$\frac{1}{D_{A,g}} = \frac{1}{D_{A,b}} + \frac{1}{D_{A,Kn}} \tag{25}$$

where the Knudsen diffusion depends on the pore diameter, the temperature, and the molecular weight of the gas[45]

$$D_{Kn} = \frac{1}{3} d_p \sqrt{\frac{8RT}{\pi M_A}} \tag{26}$$

where d_p is the pore diameter (m), R is the gas constant (J $kmol^{-1}$ K^{-1}), T is the temperature (K), and M_A is the molecular weight of the gas (g mol^{-1}). Diffusivity is obtained in squared meters per second.

The diffusion coefficient of a gas into a common solvent can be estimated using the Wilke−Chang correlation.[46]

Table 6. Operational Conditions Used to Carry out the Performance Comparison between the Tubular Membrane Contactor and the Transverse Flow Membrane Contactor

ionic liquid	$BMImBF_4$
gas flow rate (mL min^{-1})	1600
gas pressure (bar)	1
inlet gas composition (%v/v C_3H_6/C_3H_8)	50/50
liquid flow rate (mL min^{-1})	1000
liquid pressure (bar)	1.2
$[Ag^+]$ (mol L^{-1})	0.1
temperature (K)	298

$$D_{A,B} = \frac{7.4 \times 10^{-8} (\varnothing_B M_B)^{1/2} T}{\mu_B V_A^{0.6}} \tag{27}$$

where A and B refer to the gas and the absorption liquid respectively. $\varnothing_B$ is the association factor for the solvent; M_B is the molecular weight of the solvent (g mol^{-1}); T is the temperature (K); μ_B is the solvent viscosity (cP); V_A is the molar volume of the gas at its normal boiling temperature (cm^3 mol^{-1}). Diffusivity is obtained in squared centimeters per second.

Although the Wilke−Chang equation provides good results in the estimation of diffusion coefficients in common solvents, it is not suitable to calculate the diffusion coefficients in more complex solvents such as ionic liquids. In that case the diffusion coefficient of a gas can be estimated using the correlation developed by Scovazzo and co-workers for imidazolium-based ionic liquids[47]

$$D_{AB} = 2.66 \times 10^{-3} \frac{1}{\mu_B^{0.66 \pm 0.03} V_A^{1.04 \pm 0.08}} \tag{28}$$

where A and B refer to solute and solvent, respectively. μ_B is viscosity in centipoise, V_A is the molar volume of the gas in cubic centimeters per mole, and the diffusivity is obtained in squared centimeters per second.

2.4. Chemical Reaction. Once the gas is absorbed into the liquid according to Henry's law, it could be able to react with an absorbent agent S present in the liquid phase (reaction a).

$$A + S \overset{K_{Eq,1}}{\longleftrightarrow} AS \tag{a}$$

Therefore, the equilibrium constant can be defined as follows

$$K_{Eq,1} = \frac{[AS]}{[A][S]} \tag{29}$$

dx.doi.org/10.1021/ie302614r | Ind. Eng. Chem. Res. 2013, 52, 8843−8855

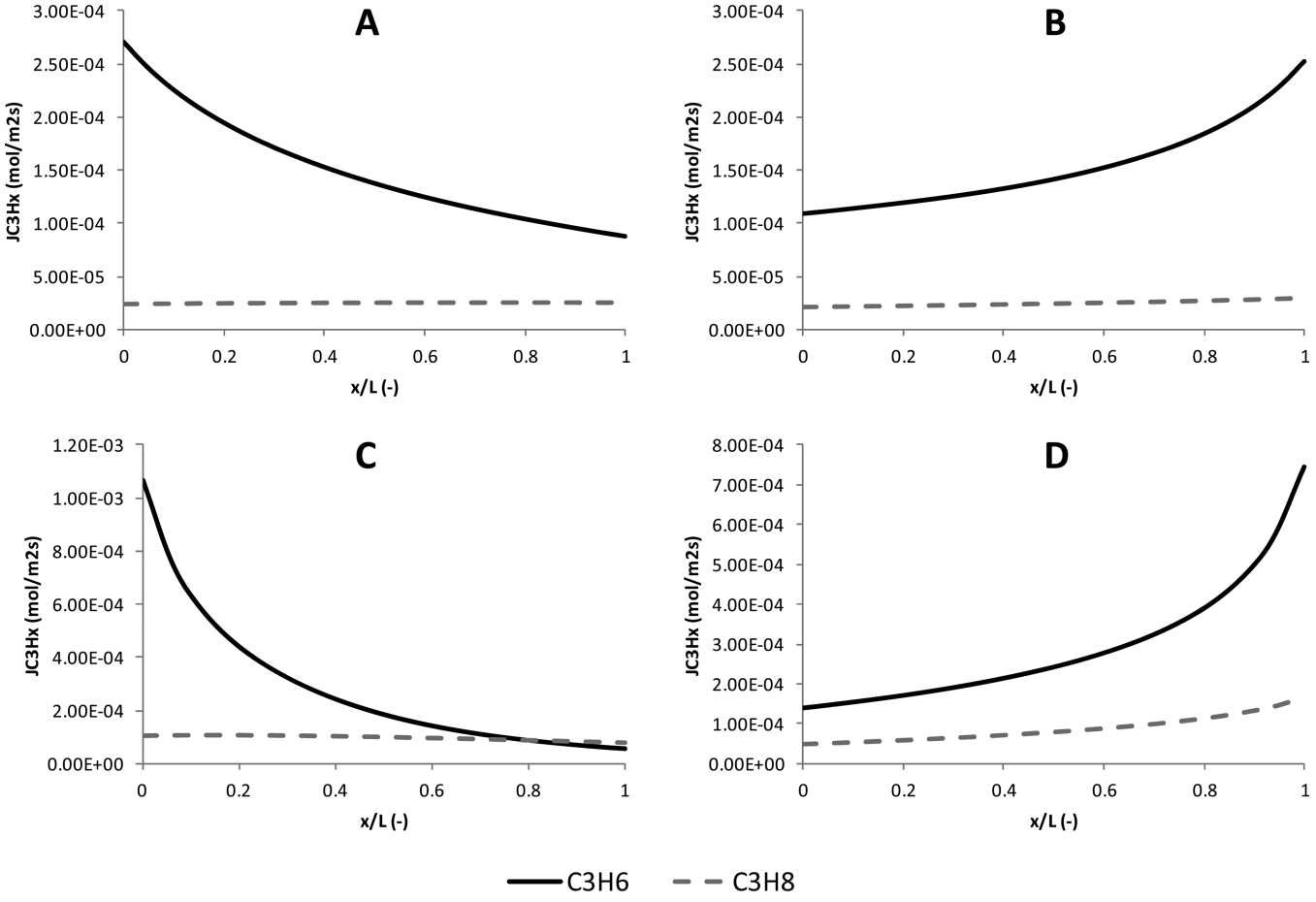

Figure 7. Evolution of absorption fluxes of propane and propylene with the dimensionless position in the membrane contactor: (A) tubular membrane contactor with gas and liquid flowing cocurrently, (B) tubular membrane contactor flowing countercurrently, (C) transverse flow membrane contactor with gas and liquid flowing cocurrently, (D) transverse flow membrane contactor flowing countercurrently.

Considering all the species of the gas A that can coexist at the same time in the liquid phase, the total concentration of gas dissolved in the reaction medium is the sum of the free gas dissolved in the liquid and the gas molecules which have been bounded by the chemical reaction.

$$[A]^T = [A] + [AS] \tag{30}$$

Similarly a mass balance for the absorbing agent S can be established.

$$[S]^T = [S] + [AS] \tag{31}$$

The dependence of the equilibrium constant with temperature can be described in most cases by the Van't Hoff equation (eq 32)

$$\frac{d\ln K}{d\left(\frac{1}{T}\right)} = -\frac{\Delta H_r}{R} \tag{32}$$

where T is the temperature in kelvin, ΔH_r is the enthalpy of the reaction (kJ mol^{-1}), and R is the gas constant (kJ mol^{-1} K^{-1}).

Moreover, the chemical reaction which takes place between the gas and the solvent can enhance the absorption flux through the enhancement factor which increases the overall mass transfer coefficient. This enhancement factor (E_A) is defined as the ratio of the absorption flux of a gas in the liquid in the presence of a chemical reaction to the absorption flux in the absence of a reaction referring these fluxes to the same driving force.

$$E_A = \frac{J_A \text{ with reaction}}{J_A \text{ without reaction}} \tag{33}$$

In this work the enhancement factor has been calculated using the approximated solution proposed by DeCoursey for absorption with irreversible second-order reaction.[48]

$$E_A = -\frac{Ha^2}{2(E_{A\infty} - 1)} + \sqrt{\frac{Ha^2}{4(E_{A\infty} - 1)^2} + \frac{E_{A\infty} Ha^2}{(E_{A\infty} - 1)} + 1} \tag{34}$$

where Ha is the Hatta number which relates the maximum conversion in the film and the maximum mass transport through the film and $E_{A\infty}$ is the infinite enhancement factor which can be calculated using the asymptotic solution proposed by Danckwerts (eqs 35 and 36).[49]

$$Ha^2 = \frac{\frac{2}{n+1} k_{1,1} (C_A^{int,L})^{n-1} C_S^m D_{A,l}}{k_l^2} \tag{35}$$

$$E_{A\infty} = \left(1 + \frac{D_S C_S}{D_{A,l} C_A^{int,L}}\right)\left(\frac{D_{A,l}}{D_S}\right)^{0.5} \tag{36}$$

dx.doi.org/10.1021/ie302614r | Ind. Eng. Chem. Res. 2013, 52, 8843−8855

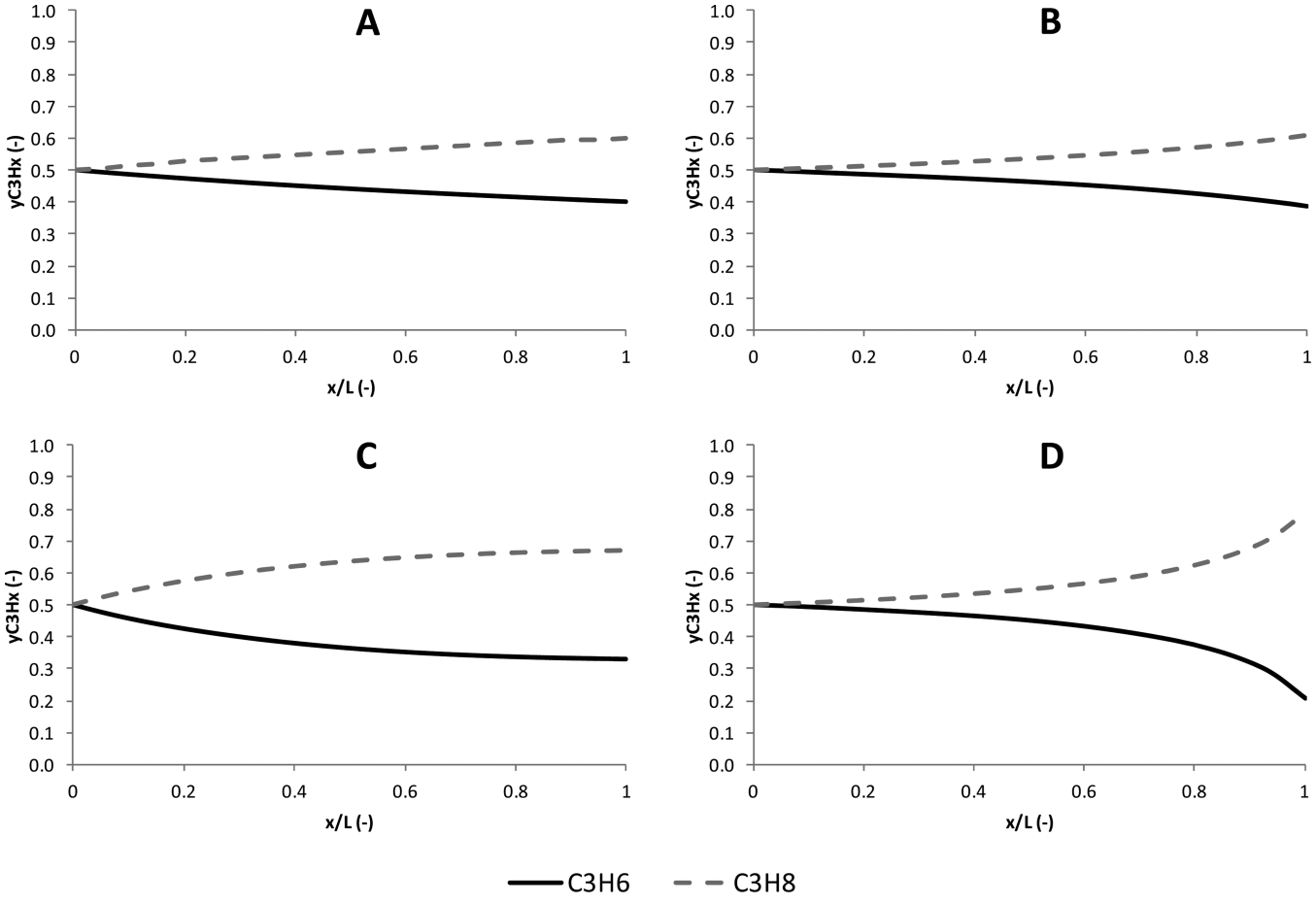

Figure 8. Evolution of molar fractions of propane and propylene with the dimensionless position in the membrane contactor: (A) tubular membrane contactor with gas and liquid flowing cocurrently, (B) tubular membrane contactor flowing countercurrently, (C) transverse flow membrane contactor with gas and liquid flowing cocurrently, (D) transverse flow membrane contactor flowing countercurrently.

3. VALIDATION OF THE MATHEMATICAL MODEL

In this section, first we will validate the mathematical model described above comparing the model prediction with experimental data previously reported by our group. Then, the model will be used to make a comparative study of the performance of the absorption process working with different membrane contactor configurations (parallel flow or cross-flow) and flow mode (cocurrent or countercurrent flow). We have chosen the propane−propylene separation as a case study. The C3 separation is currently performed by distillation, but the relative volatility, however, is very low, making the distillation difficult and expensive. In recent years, our research group has proposed to carry out the separation by reactive absorption of the propylene by mixtures based on ionic liquids containing dissolved silver salts.[50] It has been reported that the use of suitable Ag^+−room temperature ionic liquid (RTIL) mixtures as reaction media in the separation of propylene−propane mixtures improves the efficiency for propylene absorption because the silver cation becomes chemically more active in forming silver−olefin complexes. In this process, it is highly desirable that the hydrophobicity of the membrane is high enough to avoid membrane wetting (i.e., filling of membrane micropores with the liquid solution), so as to minimize the mass transfer resistance in the membrane, and therefore, polypropylene hollow fibers have been used for experiments.

The mathematical model previously described is applied to predict the separation of propane−propylene gas mixtures by reactive absorption using a silver tetrafluoroborate solution in 1-butyl-3-methyl imidazolium tetrafluoroborate ($BMImBF_4$) as absorption medium in membrane contactors. Figure 2 depicts the propane and propylene gas absorption mechanism with the resistances in series approach in a nonwetted membrane contactor.

The reactive capture of C_3H_6 with a RTIL-based solvent that contains silver(I) ions can proceed with the formation of the primary reversible π-complex between the C_3H_6 and the silver ions, and it is described by the following reaction:

$$Ag^+ + C_3H_6 \leftrightarrow Ag^+(C_3H_6) \qquad \text{primary complexation} \qquad \text{(reaction 1)}$$

The secondary complex is formed through a consecutive reaction of the primary complex with another propylene molecule:

$$Ag^+(C_3H_6) + C_3H_6 \leftrightarrow Ag^+(C_3H_6)_2$$

$$\text{secondary complexation} \qquad \text{(reaction 2)}$$

The equilibrium constants are defined as

$$K_{Eq,1} = \frac{|Ag^+(C_3H_6)|}{[Ag^+][C_3H_6]},$$

$$K_{Eq,2} = \frac{|Ag^+(C_3H_6)_2|}{[Ag^+(C_3H_6)][C_3H_6]} \qquad \text{(37a,b)}$$

Due to the high viscosity of the ionic liquid mixtures, they flow preferably through the shell side and the gas mixture flows through the lumen of the fibers, to prevent a high pressure drop.

dx.doi.org/10.1021/ie302614r | Ind. Eng. Chem. Res. 2013, 52, 8843−8855

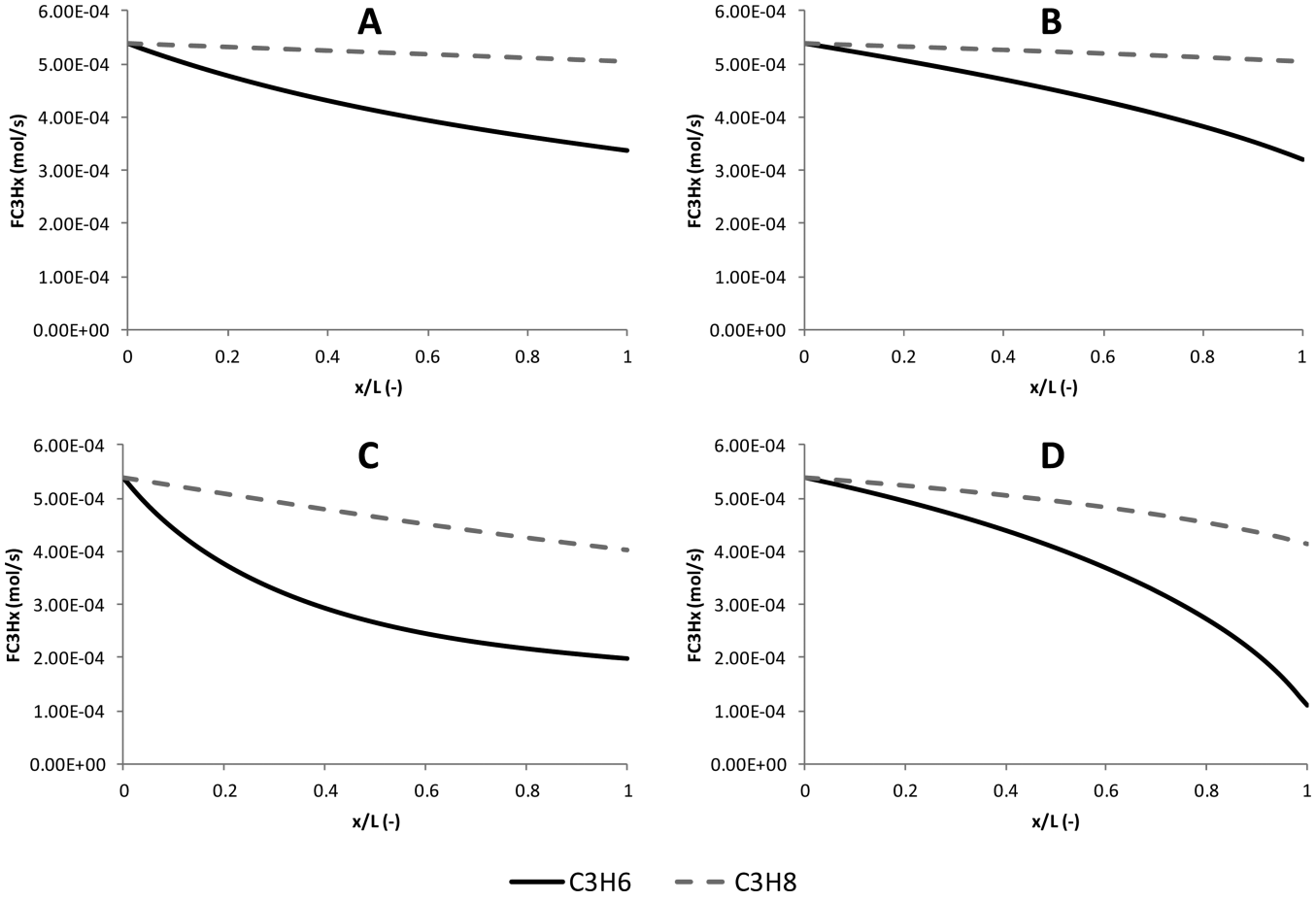

Figure 9. Evolution of molar flow rates of propane and propylene with the dimensionless position in the membrane contactor: (A) tubular membrane contactor with gas and liquid flowing cocurrently, (B) tubular membrane contactor flowing countercurrently, (C) transverse flow membrane contactor with gas and liquid flowing cocurrently, (D) transverse flow membrane contactor flowing countercurrently.

The values of the parameters and properties used in the simulation (Table 2) were obtained using the different correlations reported in the literature[29,30,43−45,47] or from the fitting to the experimental values previously reported by our research group.[51−54]

Once the model was developed, a simulation analysis was performed in order to check the model sensitivity under different operational conditions such as different feed gas compositions in the range 30%/70% propylene, different liquid flow rates between 300 and 900 mL/min, and different silver concentrations from 0 up to 0.25 M. In order to solve the mathematical model, the above model equations were implemented in Aspen Custom Modeler using its object-oriented modeling language. To enable a comparison of the various studied configurations, model simulations have been made under steady state conditions. The membrane contactor used for model validation was a parallel flow membrane contactor with tubular configuration. The main characteristics of the module are summarized in Table 3. The parallel flow membrane contactor with tubular configuration has low interfacial area which combined with the less favorable hydrodynamics for mass transport in the shell side results in a pseudosteady state where the liquid is very far from saturation. Therefore the mathematical model was validated considering this pseudosteady state. On the contrary, the much higher gas fluxes obtained with the cross-flow membrane contactor together with the higher membrane area force a fast liquid saturation leading to a dynamic state where the flux and the module outlet gas composition rapidly change with time, making it difficult to validate the model. Nevertheless, the only difference between both contactors lies in the fluid dynamics through the shell side

In this section, the mathematical model was validated using the experimental data previously reported by Ortiz et al.[51−55] These experiments were performed under the same operation conditions defined to carry out the simulation analysis (Table 4) and following the experimental procedure described by the authors in a previous work.

Figures 3−5 show the comparison between experimental and simulated data in terms of gas composition at the outlet of the parallel flow membrane contactor with tubular configuration (MICRODYN MD020 TP 2N) with gas and liquid phases flowing in counter current mode, under different conditions. Upon the basis of the comparison, it can be confirmed that there is a good agreement between the experimental results and simulated data.

Figure 3 depicts the effect of the silver salt concentration in the absorbing mixture, clearly showing that the separation efficiency improves with an increase in the concentration of silver. For a feed composition of 50% v/v of C_3H_6/C_6H_8 in the parallel flow membrane contactor, the propylene flux is strongly enhanced from 1.59×10^{-5} to 3.46×10^{-5} mol m^{-2} s^{-1} when the silver salt is added up to 0.1 M of concentration in the ionic liquid $BMImBF_4$. However when the silver ion concentration

dx.doi.org/10.1021/ie302614r | Ind. Eng. Chem. Res. 2013, 52, 8843−8855

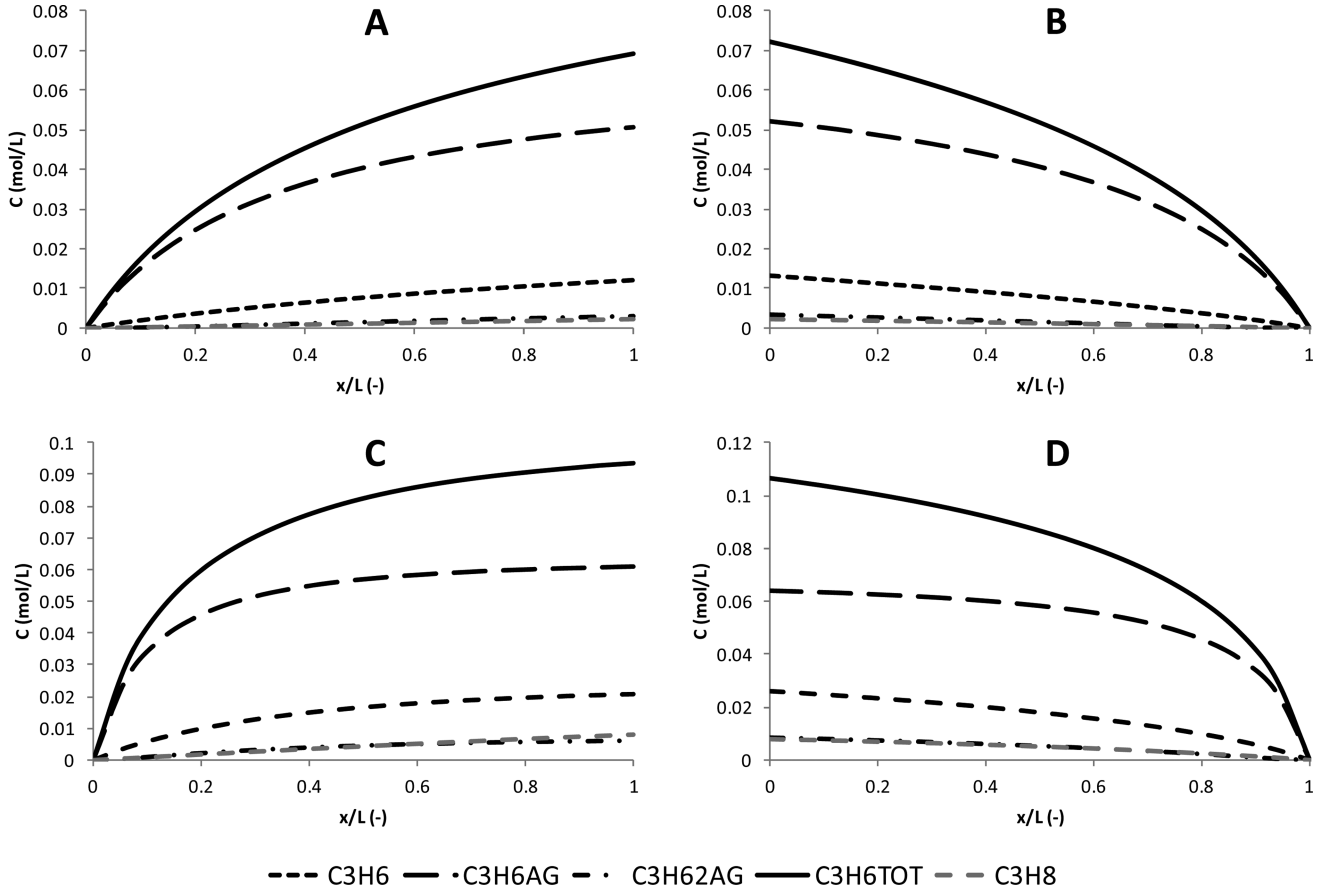

Figure 10. Evolution of the concentration of free propane, free propylene, first complex, second complex, and total propylene in the liquid phase with the dimensionless position in the membrane contactor: (A) tubular membrane contactor with gas and liquid flowing cocurrently, (B) tubular membrane contactor flowing countercurrently, (C) transverse flow membrane contactor with gas and liquid flowing cocurrently, (D) transverse flow membrane contactor flowing countercurrently.

increases from 0.1 to 0.25 M, the enhancement on the propylene flux is negligible. This phenomenon could be attributed to the strong dependency of the viscosity of the $Ag^{+}-BMImBF_4$ reactive medium with the silver ions concentration that induces gas diffusion rate limitations.

Since for the studied conditions the main resistance to mass transport is located in the liquid phase, the absorbent liquid flow rate has a great influence on the separation efficiency, as shown in Figure 4. This phenomenon is attenuated with the transverse flow membrane contactor where the diffusion rate limitations are strongly improved. Figure 5 also shows the good agreement between the experimental data and model predictions for various feed gas compositions and different silver salt contents in the ionic liquid absorbing mixtures.

4. SIMULATION AND PREDICTION OF PROCESS CONDITIONS

Once the mathematical model previously developed has been validated, it has been used to compare the performance of a conventional tubular membrane contactor and a transverse flow membrane contactor in the separation process using different flowing configurations as it can be seen in Figure 6. Both modules were compared considering the same membrane area (1.4 m^2) with the gas and liquid phases flowing in cocurrent flow and also countercurrently. Table 5 summarizes the parameters of the membrane modules used to make the comparison.

The operational conditions used to carry out the comparison of the two different membrane contactors are shown in Table 6. In the proposed case study, the liquid absorbents (ionic liquid mixtures) have a high viscosity, and as a consequence, the controlling mass transfer resistance is located in the liquid phase boundary layer. Therefore, it is very important that a suitable correlation is used to estimate the mass transfer coefficients. In this work, the correlations proposed by Wu and Chen (eq 13, parallel flow module) and Fallanza et al. (eq 21, transverse flow contactor) have been used to predict the mass transfer coefficient in the liquid flowing through the shell after the accurate predictions of the experimental behavior that have been reported formerly.[41,55] Mass transfer coefficients in the gas phase for lumen-side laminar flow and low *Gz* numbers were calculated using the Hausen equation (eq 7). A general conclusion is that unless the liquid film coefficients were very large or the membrane suffered from partial pore filling with the absorbent liquid, the membrane resistance was not significant.[55]

Figures 7−11 show the simulated results using a parallel flow membrane contactor with tubular configuration and a transverse flow hollow fiber membrane contactor for the gas and liquid phases flowing cocurrently and countercurrently. Results are presented as the profiles of the different variables under study (flux of gases across the membrane, molar flow rate of the gases, gas composition, concentration of all the species in the liquid phase, and enhancement factor) with the position inside the contactor. As expected, in membrane contactors, the

dx.doi.org/10.1021/ie302614r | *Ind. Eng. Chem. Res.* 2013, 52, 8843−8855

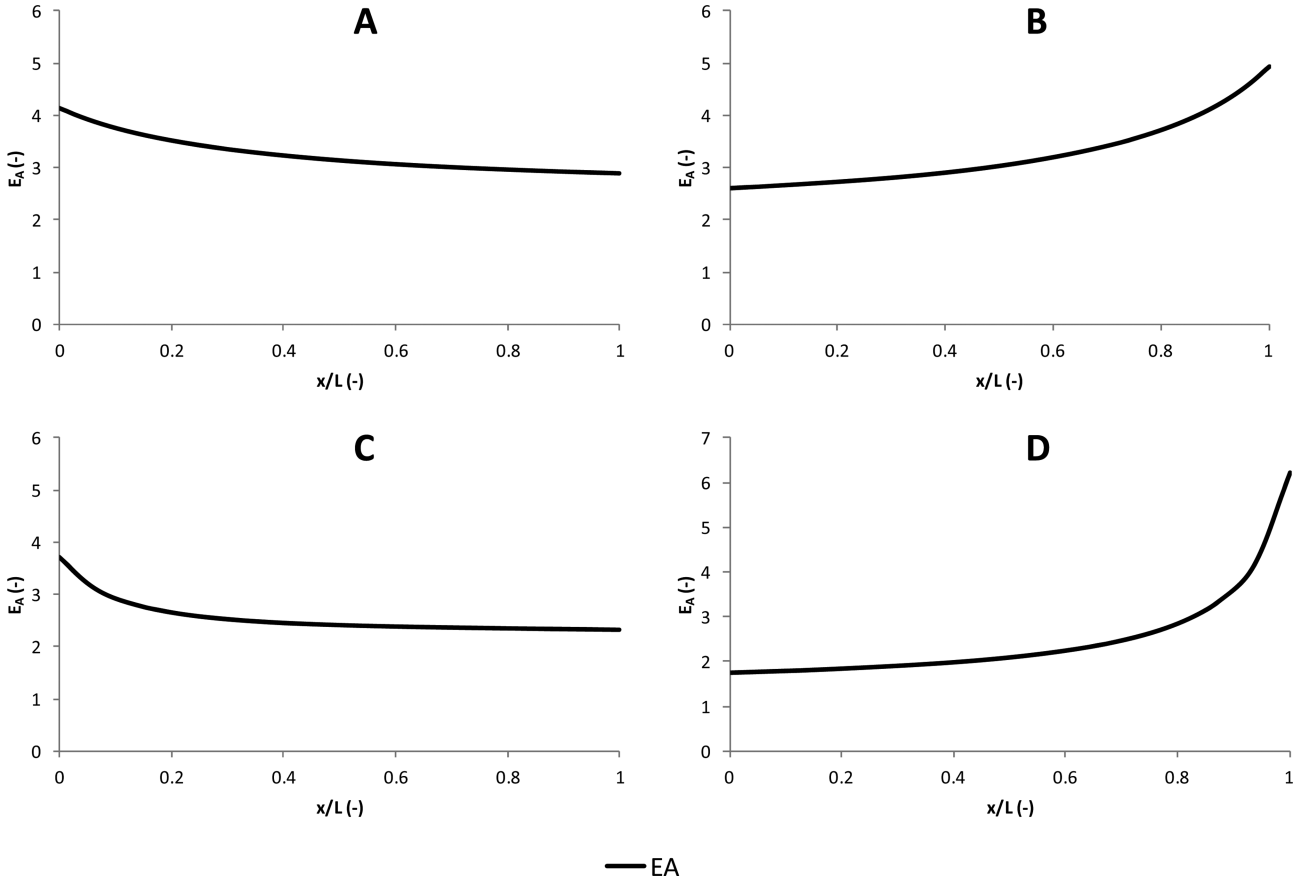

Figure 11. Evolution of the enhancement factor with the dimensionless position in the membrane contactor: (A) tubular membrane contactor with gas and liquid flowing cocurrently, (B) tubular membrane contactor flowing countercurrently, (C) transverse flow membrane contactor with gas and liquid flowing cocurrently, (D) transverse flow membrane contactor flowing countercurrently.

countercurrent flow mode provided better results than those obtained with the gas and liquid phases flowing cocurrently. On the other hand, it can be noted that the improved fluid dynamics of the transverse flow membrane contactor provided higher fluxes of both gases across the membrane, resulting in a better separation of the gas stream. This is mainly because in the proposed case study the main resistance to the mass transfer is located in the liquid phase boundary layer. Parallel flow offers the highest average concentration driving force in the case of countercurrent flow and is preferred in situations where membrane or fiber side mass transfer resistance controls. Moreover, the hollow fiber configuration of the transverse flow membrane contactor allows a membrane area of 1.4 m^2 in a total volume of 0.314×10^{-3} m^3 to be held, while when using a tubular configuration, a volume of equipment 28.5 times higher (8.97×10^{-3} m^3) is needed.

5. CONCLUSIONS

In this work a simple mathematical model able to describe the mass transfer rate of a reactive absorption process carried out in a gas−liquid membrane contactor is provided. Being the hollow fiber module the configuration of major interest for industrial applications, particular attention is devoted to it. This work includes a theoretical section, that consist in the development of a mathematical model to describe the behavior of hollow fiber membrane contactors, and then, the proposed model was used to assess the performance of modules with different configurations (parallel flow or cross-flow devices) and different flow mode (counter-current and cocurrent flow). Reliability of the proposed model was checked by comparison of the model prediction with experimental results previously reported. It follows from the model simulation that system performance can be improved by operating a module in an appropriate flow mode (counter-flow). Furthermore, the absorption rate is significantly improved by the use of a cross-flow module, due to the remarkable increase of the mass transfer coefficient in the liquid phase circulating on the shell side.

AUTHOR INFORMATION

Corresponding Author

*Tel.: +34942201585. Fax: +34942201591. E-mail: ortizi@unican.es.

Notes

The authors declare no competing financial interest.

ACKNOWLEDGMENTS

This research has been funded by the Spanish Ministry of Science and Innovation (Project CTQ2008-00690/PPQ). Marcos Fallanza also thanks MICINN for the FPI fellowship.

NOMENCLATURE

A = effective membrane area (m^2)
C = concentration (mol m^{-3})
D = diffusivity (m^2 s^{-1})
d_{out} = outer diameter of the fiber (m)
d_{in} = inner diameter of the fiber (m)

d_{cin} = inner diameter of the module (m)
d_{co} = outer diameter of the central delivery tube (m)
d_h = hydraulic diameter of the shell side (m)
d_{lm} = logarithmic mean diameter of the fiber (m)
d_p = pore diameter (m)
E_A = enhancement factor (−)
$E_{A\infty}$ = infinite enhancement factor (−)
F = gas molar flow (mol s^{-1})
J = molar flux (mol m^{-2} s^{-1})
K_{Eq} = equilibrium constant (m^3 mol^{-1})
$k_{1,1}$ = kinetic constant of reaction 1,1 order (m^3 mol^{-1} s^{-1})
k_g = mass transfer coefficient in the gas phase (m s^{-1})
k_{mg} = mass transfer coefficient in the membrane with the pores filled of gas (m s^{-1})
k_l = mass transfer coefficient in the liquid phase (m s^{-1})
$K_{overall}$ = overall mass transfer coefficient (m s^{-1})
H = Henry's constant (mol m^{-3} bar^{-1})
H_{di} = dimensionless Henry's constant (−)
ΔH_{sol} = standard solvation enthalpy (kJ mol^{-1})
N = number of fibers of the membrane module
L = effective fiber length (m)
P = pressure (bar)
Q_L = liquid flow rate (m^3 s^{-1})
R = universal gas constant (kJ mol^{-1} K^{-1})
T = temperature (K)
u_e = mean superficial velocity of the liquid (m s^{-1})
V = volume (m^3)
y = gas molar fraction (−)
z = axial distance (m)

Dimensionless Numbers

Gz = Graetz number (−)
Ha = Hatta number (−)
Sh = Sherwood number (−)
Sc = Schmidt number (−)
Re = Reynolds number (−)

Greek Letters

δ = membrane thickness (m)
ε = porosity of the membrane (−)
μ = viscosity (Pa s)
ν = kinematic viscosity (m^2 s^{-1})
τ = tortuosity (−)
ρ = density (kg m^{-3})

Superscripts/Subscripts

Ag^+ = silver ion
C_3H_6 = propylene
C_3H_8 = propylene

REFERENCES

(1) Hamborg, E. S.; Versteeg, G. F. Absorption and desorption mass transfer rates in chemically enhanced reactive systems. Part I: Chemical enhancement factors. *Chem. Eng. J.* **2012**, *198*−*199*, 555−560.

(2) Dindore, V. Y. Gas purification using membrane gas absorption processes, PhD Dissertation. University of Twente, The Netherlands, 2003.

(3) Drioli, E.; Criscuoli, A.; Curcio, E. *Membrane Contactors: Fundamentals, Applications and Potentialities*; Elsevier: Amsterdam, 2006.

(4) Gabelman, A.; Hwang, S. T. Hollow fiber membrane contactors. *J. Membr. Sci.* **1999**, *159*, 61−106.

(5) Mansourizadeh, A.; Ismail, A. F. Hollow fiber gas−liquid membrane contactors for acid gas capture: A review. *J. Hazard. Mater.* **2009**, *171*, 38−53.

(6) Atchariyawut, S.; Jiraratananon, R.; Wang, R. Mass transfer study and modeling of gas−liquid membrane contacting process by multistage cascade model for CO_2 absorption. *Sep. Purif. Technol.* **2008**, *63*, 15−22.

(7) Reed, B. W.; Semmens, M. J.; Cussler, E. L. Membrane contactors. In *Membrane Science and Technology*; Noble, R. D., Stern, S. A., Eds.; Elsevier: Amsterdam, 1995; pp 467−498.

(8) Albrecht, W.; Hilke, R.; Kneifel, K.; Weigel, T.; Peinemann, K. -V. Selection of microporous hydrophobic membranes for use in gas/liquid contactors: An experimental approach. *J. Membr. Sci.* **2005**, *263*, 66−76.

(9) Korikov, A. P.; Sirkar, K. K. Membrane gas permeance in gas-liquid membrane contactor systems for solutions containing a highly reactive absorbent. *J. Membr. Sci.* **2005**, *246*, 27−37.

(10) Stanojevic, M.; Lazarevic, B.; Radic, D. Review of membrane contactors designs and applications of different modules in industry. *FME Trans.* **2003**, *31*, 91−98.

(11) Simons, K.; Nijmeijer, K.; Wessling, M. Gas−liquid membrane contactors for CO_2 removal. *J. Membr. Sci.* **2009**, *340*, 214−220.

(12) Albo, J.; Luis, P.; Irabien, A. Carbon dioxide capture from flue gases using a cross-flow membrane contactor and the ionic liquid 1-ethyl-3-methylimidazolium ethylsulfate. *Ind. Eng. Chem. Res.* **2010**, *49*, 11045−11051.

(13) Qi, Z.; Cussler, E. L. Microporous hollow fibers for gas absorption: I. Mass transfer in the liquid. *J. Membr. Sci.* **1985**, *23*, 321−332.

(14) Rongwong, W.; Jiraratananon, R.; Atchariyawut, S. Experimental study on membrane wetting in gas-liquid membrane contacting process for CO_2 absorption by single and mixed absorbents. *Sep. Purif. Technol.* **2009**, *69*, 118−125.

(15) Boucif, N.; Corriou, J. P.; Roizard, D.; Favre, E. Carbon dioxide absorption by monoethanolamine in hollow fiber membrane contactors: A parametric investigation. *AIChE J.* **2012**, *58*, 2843−2855.

(16) Luis, P.; Van Gerven, T.; Van der Bruggen, B. Recent developments in membrane-based technologies for CO_2 capture. *Prog. Energy Combust. Sci.* **2012**, *38*, 419−448.

(17) Wang, D.; Teo, W. K.; Li, K. Selective removal of trace H_2S from gas streams containing CO_2 using hollow fibre membrane modules/contractors. *Sep. Purif. Technol.* **2004**, *35*, 125−131.

(18) Luis, P.; Garea, A.; Irabien, A. Zero solvent emission process for sulfur dioxide recovery using a membrane contactor and ionic liquids. *J. Membr. Sci.* **2009**, *330*, 80−89.

(19) Park, H. H.; Deshwal, B. R.; Kim, I. W.; Lee, H. K. Absorption of SO_2 from flue gas using PVDF hollow fiber membranes in a gas-liquid contactor. *J. Membr. Sci.* **2008**, *319*, 29−37.

(20) Klaassen, R.; Feron, P. H. M.; Jansen, A. E. Membrane contactors in industrial applications. *Chem. Eng. Res. Des.* **2005**, *83*, 234−246.

(21) Karoor, S.; Sirkar, K. K. Gas absorption studies in microporous hollow fiber membrane modules. *Ind. Eng. Chem. Res.* **1993**, *32*, 674−684.

(22) Kreulen, H.; Smolders, C. A.; Versteeg, G. F.; Van Swaaij, W. P. M. Microporous hollow fibre membrane modules as gas-liquid contractors. Part 2. Mass transfer with chemical reaction. *J. Membr. Sci.* **1993**, *78*, 217−238.

(23) Keshavarz, P.; Ayatollahi, S.; Fathikalajahi, J. Mathematical modeling of gas−liquid membrane contactors using random distribution of fibers. *J. Membr. Sci.* **2008**, *325*, 98−108.

(24) Chilukuri, P.; Rademakers, K.; Nymeijer, K.; Van der Ham, L.; Van Berg, H. D. Propylene/propane separation with a gas/liquid membrane contactor using a silver salt solution. *Ind. Eng. Chem. Res.* **2007**, *46*, 8701−8709.

(25) Astarita, G. *Mass transfer with chemical reaction*; Elsevier Publishing Company: Amsterdam, 1967.

(26) Hiwale, R.; Hwang, S.; Smith, R. Model building methodology for multiphase reaction systems-modeling of CO_2 absorption in monoethanolamine for laminar jet absorbers and packing beds. *Ind. Eng. Chem. Res.* **2012**, *51*, 4328−4346.

(27) Yang, D.; Barbero, R. S.; Devlin, D. J.; Cussler, E. L.; Colling, C. W.; Carrera, M. E. Hollow fibers as structured packing for olefin/paraffin separations. *J. Membr. Sci.* **2006**, *279*, 61−69.
(28) Sirkar, K. K. Membranes, phase interfaces, and separations: Novel techniques and membranes-an overview. *Ind. Eng. Chem. Res.* **2008**, *47*, 5250−5266.
(29) Skelland, A. H. P. *Diffusional mass transfer*; John Wiley & Sons: New York, 1974.
(30) Perry, R. H.; Green, D. W.; Maloney, J. O. *Perry's chemical engineers' handbook*; McGraw-Hill: New York, 1997.
(31) Yang, M.; Cussler, E. L. Designing hollow-fiber contactors. *AIChE J.* **1986**, *32*, 1910−1916.
(32) Prasad, R.; Sirkar, K. K. Dispersion-free solvent extraction with microporous hollow-fiber modules. *AIChE J.* **1988**, *34*, 177−188.
(33) Wu, J.; Chen, V. Shell-side mass transfer performance of randomly packed hollow fiber modules. *J. Membr. Sci.* **2000**, *172*, 59−74.
(34) Costello, M. J.; Fane, A. G.; Hogan, P. A.; Schofield, R. W. The effect of shell side hydrodynamics on the performance of axial flow hollow fibre modules. *J. Membr. Sci.* **1993**, *80*, 1−11.
(35) Li, K.; Tai, M. S. L.; Teo, W. K. Design of a CO_2 scrubber for self-contained breathing systems using a microporous membrane. *J. Membr. Sci.* **1994**, *86*, 119−125.
(36) Zheng, J.; Dai, Z.; Wong, F.; Xu, Z. Shell side mass transfer in a transverse flow hollow fiber membrane contactor. *J. Membr. Sci.* **2005**, *261*, 114−120.
(37) Fouad, E. A.; Bart, H. J. Separation of zinc by a non-dispersion solvent extraction process in a hollow fiber contactor. *Solvent Extr. Ion Exc.* **2007**, *25*, 857−877.
(38) Schöner, P.; Plucinski, P.; Nitsch, W.; Daiminger, U. Mass transfer in the shell side of cross flow hollow fiber modules. *Chem. Eng. Sci.* **1998**, *53*, 2319−2326.
(39) Baudot, A.; Floury, J.; Smorenburg, H. E. Liquid-liquid extraction of aroma compounds with hollow fiber contactor. *AIChE J.* **2001**, *47*, 1780−1793.
(40) Shen, S.; Kentish, S. E.; Stevens, G. W. Shell-side mass-transfer performance in hollow-fiber membrane contactors. *Solvent Extr. Ion Exc.* **2010**, *28*, 817−844.
(41) Fallanza, M.; Ortiz, A.; Gorri, D.; Ortiz, I. Improving the mass transfer rate in G−L membrane contactors with ionic liquids as absorption medium. Recovery of propylene. *J. Membr. Sci.* **2011**, *385*−*386*, 217−225.
(42) Hansen, K. C.; Zhou, Z.; Yaws, C. L.; Aminabhavi, T. M. Determination of Henry's law constants of organics in dilute aqueous solutions. *J. Chem. Eng. Data* **1993**, *38*, 546−550.
(43) Fuller, E. N.; Schettler, P. D.; Giddings, J. C. New method for prediction of binary gas-phase diffusion coefficients. *Ind. Eng. Chem.* **1966**, *58*, 18−27.
(44) Satterfield, C. *Mass transfer in heterogeneous catalysis*; MIT Press: Cambridge, MA, 1970.
(45) Cussler, E. L. *Diffusion: Mass Transfer in Fluid Systems*, 3rd ed.; Cambridge University Press: New York, 2009.
(46) Wilke, C. R.; Chang, P. Correlation of diffusion coefficients in dilute solutions. *AIChE J.* **1955**, *1*, 264−270.
(47) Morgan, D.; Ferguson, L.; Scovazzo, P. Diffusivities of gases in room-temperature ionic Liquids: Data and correlations obtained using a lag-time technique. *Ind. Eng. Chem. Res.* **2005**, *44*, 4815−4823.
(48) DeCoursey, W. J. Absorption with chemical reaction: development of a new relation for the Danckwerts model. *Chem. Eng. Sci.* **1974**, *29*, 1867−1872.
(49) Danckwerts, P. V. *Gas-liquid reactions*; McGraw-Hill: New York, 1970.
(50) Ortiz, A. Process intensification in the separation of olefin/paraffin mixtures, PhD Dissertation. Universidad de Cantabria, Santander, Spain, 2010.
(51) Ortiz, A.; Ruiz, A.; Gorri, D.; Ortiz, I. Room temperature ionic liquid with silver salt as efficient reaction media for propylene/propane separation: Absorption equilibrium. *Sep. Purif. Technol.* **2008**, *63*, 311−318.
(52) Ortiz, A.; Galán Sanchez, L. M.; Gorri, D.; De Haan, A. B.; Ortiz, I. Reactive ionic liquid media for the separation of propylene/propane gaseous mixtures. *Ind. Eng. Chem. Res.* **2010**, *49*, 7227−7233.
(53) Ortiz, A.; Galán, L. M.; Gorri, D.; de Haan, A. B.; Ortiz, I. Kinetics of reactive absorption of propylene in RTIL-Ag^+ media. *Sep. Purif. Technol.* **2010**, *73*, 106−113.
(54) Fallanza, M.; Ortiz, A.; Gorri, D.; Ortiz, I. Effect of liquid flow on the separation of propylene/propane mixtures with a gas/liquid membrane contactor using Ag^+-RTIL solutions. *Desalin. Water Treat.* **2011**, *27*, 123−129.
(55) Ortiz, A.; Gorri, D.; Irabien, Á.; Ortiz, I. Separation of propylene/propane mixtures using Ag^+−RTIL solutions. Evaluation and comparison of the performance of gas−liquid contactors. *J. Membr. Sci.* **2010**, *360*, 130−141.